Colloid Polym Sci 278:443–449 (2000)

ORIGINAL CONTRIBUTION

M. Ocaña

Uniform particles of manganese compounds obtained by forced hydrolysis of manganese(II) acetate

Received: 19 October 1999
Accepted: 24 November 1999

M. Ocaña (✉)
Instituto de Ciencia de Materiales de Sevilla (CSIC-UNSE), Americo Vespucio s/n, Isla de La Cartuja
41092 Sevilla, Spain

Abstract Procedures for the preparation at low temperature (80 °C) of uniform colloids consisting of Mn_3O_4 nanoparticles (about 20 nm) or elongated α-MnOOH particles with length less than 2 μm and width 0.4 μm or less, based on the forced hydrolysis of aqueous manganese(II) acetate solutions in the absence (Mn_3O_4) or the presence (α-MnOOH) of HCl are described. These solids are only produced under a very restrictive range of reagent concentrations involving solutions of 0.2–0.4 mol dm^{-3} manganese(II) acetate for Mn_3O_4 and of 1.6–2 mol dm^{-3} Mn(II) and 0.2–0.3 mol dm^{-3} HCl for α-MnOOH. The role that the acetate anions play in the precipitation of these solids is analyzed. It seems that these anions promote the oxidation of Mn(II) to Mn(III), which readily hydrolyze causing precipitation. The evolution of the characteristics of the powders with temperature up to 900 °C is also reported. Thus, Mn_3O_4 particles transform to Mn_2O_3 upon calcination at 800 °C; this is accompained by a sintering process. The α-MnOOH sample also experiences several phase transformations on heating. First, it is oxidized at low temperatures (250–450 °C) giving MnO_2 (pyrolusite), which is further reduced to Mn_2O_3 at 800 °C. After this process the particles still retain their elongated shape.

Key words Manganese oxide · Manganese oxyhydroxide · Uniform particles · Nanoparticles

Introduction

Manganese oxides and oxyhydroxides are of considerable importance in many technological applications. To mention a few, Mn_2O_3, Mn_3O_4 and MnO_2 have been reported to be efficient catalysts in many environmental reactions and in the synthesis of organic compounds [1–3], whereas MnO_2 electrodes are widely used in alkaline batteries [3, 5] in which MnOOH is produced during the electrochemical processes [5].

The advantages of using powdered materials with controlled particle size and shape have been amply documented [6]. The properties of such solids can also be altered if the particle size is reduced to the nanometer range [7].

Usually, MnO_2 is prepared by redox reactions involving Mn(VII) and/or Mn(II) salts [3] whereas Mn_2O_3 and Mn_3O_4 are obtained by heating manganese salts or other manganese oxides or hydroxides at about 700 °C and about 1000 °C, respectively [4, 8, 9]. Some other chemical processes have been reported for the preparation of these oxides [8, 10–11]; however, all these methods yield, in general, particles with irregular shape and broad size distribution.

The preparation of uniform particles of manganese oxides was attempted by Hamada et al. [12], who obtained spherical particles (about 5 μm) of $MnCO_3$ by aging solutions of manganese(II) sulfate and ammonium hydrogen carbonate at 50 °C. This powder was converted to $MnO_{1.8–1.9}$ by heating at 450 °C in an air

or an oxygen atmosphere after which the particle morphology was retained. More recently, Haq et al. [13] prepared cubic $MnCO_3$ particles of various modal sizes (about 0.8 μm and about 8 μm) by hydrolysis at 85 °C of manganese(II) sulfate solutions in the presence of urea, which were transformed to Mn_2O_3 on calcination at 700 °C in air, also keeping the particle shape.

This work describes procedures for the preparation at low temperature (80 °C) of equiaxial Mn_3O_4 nanoparticles and elongated α-MnOOH particles (length less than 2 μm) by forced hydrolysis of $Mn(OOCH_3)_2$ aqueous solutions in the absence or the presence of HCl, respectively. These solids were characterized in terms of their particle size and morphology, chemical composition, crystalline structure and electrokinetic behavior. Finally, the changes in the characteristics of these powders occurring on calcination up to 900 °C are also reported.

Experimental

Particle preparation

Freshly prepared aqueous solutions with the desired concentration of $Mn(OOCH_3)_2 \cdot 4H_2O$ (Aldrich, 99%) were aged for various periods of time in Pyrex test tubes tightly closed with Teflon caps placed in an oven preheated to 80 °C. After aging, the dispersions were quenched in cool water and the solids were separated from their mother liquor by centrifugation. The precipitates were then washed several times with doubly distilled water and finally dried at 50 °C before analysis.

In some experiments, HCl (Fluka, 37%) was added to the starting solutions to analyze its effects on the characteristics of the precipitated solids. The reagent concentrations were systematically varied in order to establish the appropriate conditions for the preparation of the most uniform particles.

For calcination, the powders were heated at 10 °C min^{-1} to the desired temperature, after which they were slowly cooled to room temperature.

Characterization

The morphological characteristics of the particles were examined by transmission electron microscopy (Philips 200CM). The particle size distribution was obtained by counting several hundred particles.

X-ray diffraction (Siemens D501) was used to identify the crystal structure of the samples. The IR spectra of the powders diluted in KBr were recorded using a Nicolet 510 Fourier transform IR spectrometer.

Differential thermal analysis and thermogravimetric analysis (TGA) (Setaram 92-16.18) were performed in an air atmosphere at a heating rate of 10 °C min^{-1}.

The isoelectric point, pI, of the solids was determined by measuring (Malvern Mastersizer) the electrophoretic mobilities of aqueous dispersions as a function of pH at constant ionic strength (10^{-2} mol dm^{-3} NaCl). The pH was varied by adding HCl or NaOH as needed.

Results

Particle preparation and characterization

The aging at 80 °C for 2 h of 0.4 mol dm^{-3} aqueous $Mn(OOCH_3)_2$ solutions yielded equiaxial particles such as those illustrated in Fig. 1A. The particle size analysis gave a mean diameter, d_m of 17 nm with a standard deviation, σ, of 4.5 for this sample. The corresponding histogram is shown in Fig. 2. Slightly bigger particles (d_m = 26 nm, σ = 9) with similar morphology resulted if the $Mn(OOCH_3)_2$ concentration was lowered to 0.2 mol dm^{-3}; however, at still lower concentrations more heterogeneous dispersions consisting of bigger and aggregated particles were obtained. Finally, solutions of $Mn(OOCH_3)_2$ at concentrations above 0.4 mol dm^{-3} (0.5–1 mol dm^{-3}) also yielded equiaxial particles but with much broader size distributions than those shown in Fig. 1A.

The X-ray diffraction pattern of these nanoparticles (Fig. 3) was consistent with that of Mn_3O_4 (hausmannite) [14]. In agreement, their IR spectrum (Fig. 4) only displayed three main bands (633, 527 and 415 cm^{-1}) in the region 1000-400 cm^{-1}, similar to those reported for this solid [15]. It should be noted that to our knowledge, the reaction temperature involved in the procedure described here is the lowest one reported for the synthesis of hausmannite.

The pI obtained from the electrophoretic mobility measurements for the particles shown in Fig. 1A (Fig. 5) was similar (5.7) to that previously reported for particles of mixed Mn_3O_4–Mn_2O_3 composition [16].

The addition of certain amounts (0.1–0.5 mol dm^{-3}) of HCl to 0.4 mol dm^{-3} $Mn(OOCH_3)_2$ solutions resulted in the absence of precipitation at 80 °C even if the aging was prolonged for 24 h. For higher $Mn(OOCH_3)_2$ concentrations, we obtained the precipitation domain presented in Fig. 6. As observed, most of the precipitated systems were heterogeneous, with particles of different sizes and shapes; however, for a reduced set of reagent concentrations [solutions containing 1.6–2 mol dm^{-3} $Mn(OOCH_3)$ and mostly for solutions containing 0.2–0.3 mol dm^{-3} HCl] elongated particles with length 2 μm or less width 0.4 μm or less were obtained (Fig. 1C). Owing to the heterogeneous dimensions of these particles, a detailed particle size analysis was not carried out in this case.

X-ray diffraction (Fig. 7) revealed that these elongated particles consisted of α-MnOOH (groutite) [17]. Their IR spectrum (Fig. 8) confirmed this composition, showing a doublet and a triplet at 2000 and 1000 cm^{-1}, respectively, and a broad absorption in the 2500–3000 cm^{-1} region due to the OH groups [18]. The band at about 3400 cm^{-1} and the weaker one at about 1600 cm^{-1} indicated the presence of water in the

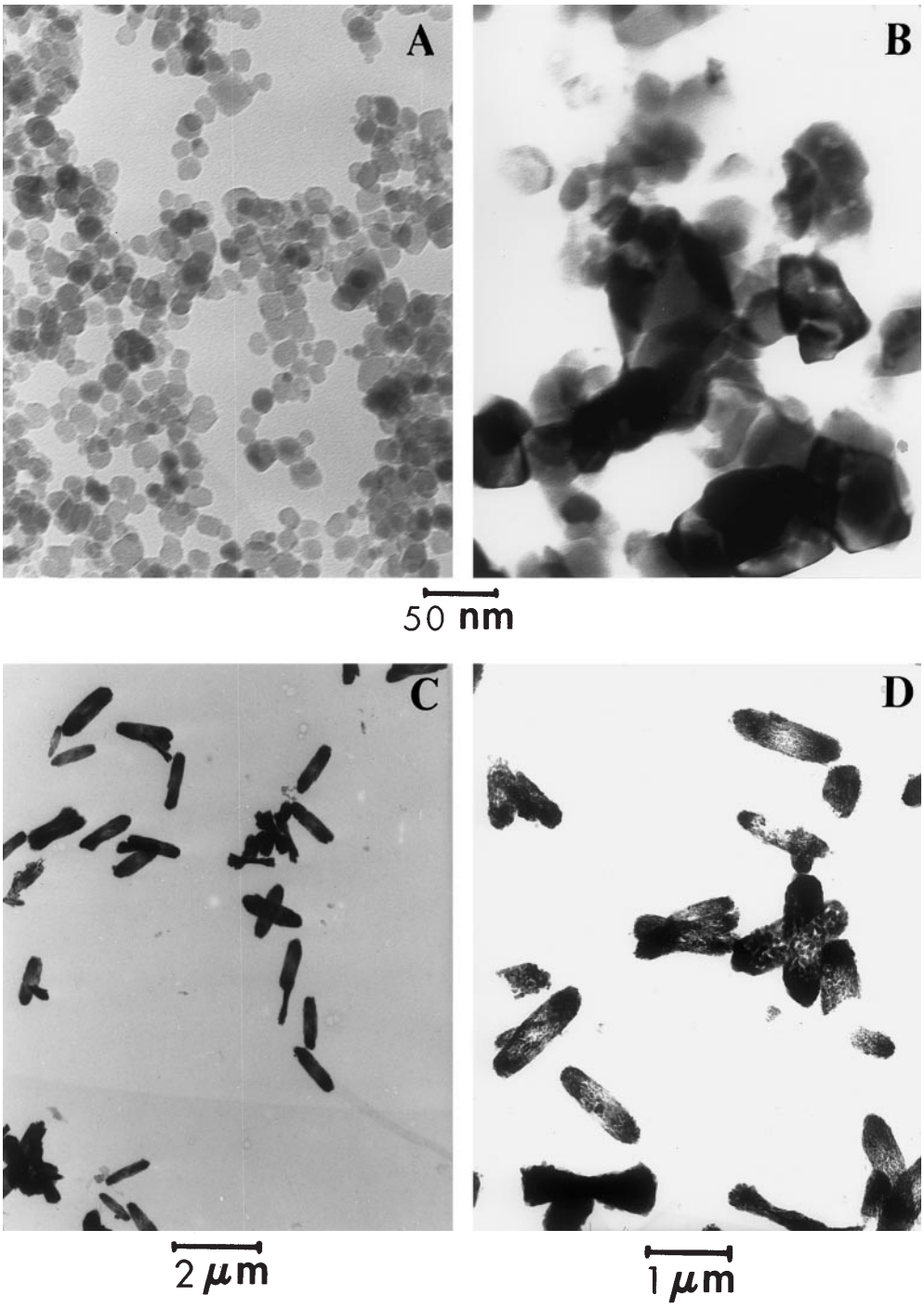

Fig. 1 Transmission electron micrographs of **A** the sample obtained by aging a 0.4 mol dm^{-3} $Mn(OOCH_3)_2$ solution at 80 °C for 2 h, **B** the sample shown in **A** heated at 800 °C, **C** the sample obtained by aging a 2 mol dm^{-3} $Mn(OOCH_3)_2$ solution in the presence of 0.2 mol dm^{-3} HCl at 80 °C for 24 h and **D** the sample shown in **C** heated at 800 °C

particles. The weak absorption at about 1400 cm^{-1} suggests that the particles may also contain a small amount of absorbed acetate [19].

The pI measured for these particles (Fig. 5) was lower (9.6) than that previously reported [20] for $Mn(OH)_2$ (12) and higher than the corresponding one for the Mn_3O_4 nanoparticles (5.7), which is in accordance with the change in particle composition.

Thermal evolution

The TGA curves obtained for the samples shown in Fig. 1A (Mn_3O_4) and C (α-MnOOH) are shown in Fig. 9. The Mn_3O_4 sample lost a small amount of weight (1.5%) between 25 and 100 °C due to the release of absorbed water. In agreement with the behavior previously reported for other Mn_3O_4 samples [10], this

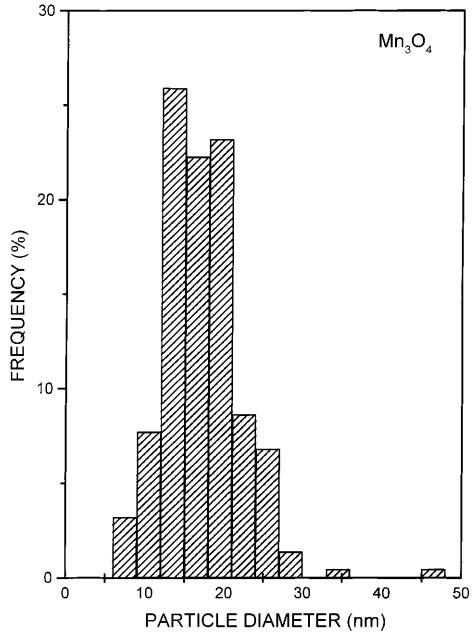

Fig. 2 Particle size histogram obtained for the Mn_3O_4 sample shown in Fig. 1A

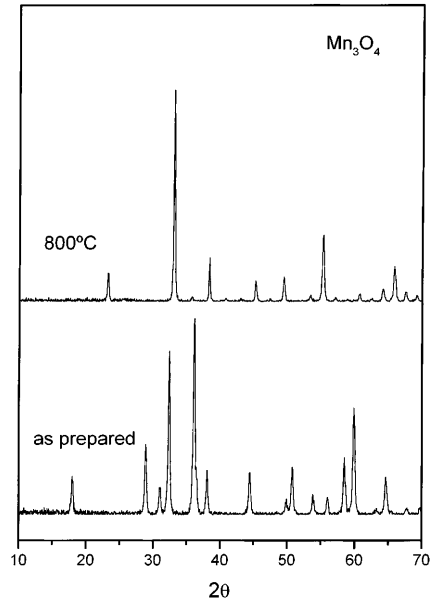

Fig. 3 X-ray diffraction patterns of the Mn_3O_4 sample shown in Fig. 1A, as prepared and after heating at 800 °C

powder also experienced a weight gain (3.3%) between 600 and 800 °C that is consistent with the oxidation of Mn_3O_4 to Mn_2O_3. This process was confirmed by the X-ray diffraction pattern of the sample heated at 800 °C (Fig. 3), which corresponded to Mn_2O_3 (bixbyite) [21]. Such a change in composition was also manifested by the IR spectrum of the sample (Fig. 4), which displayed

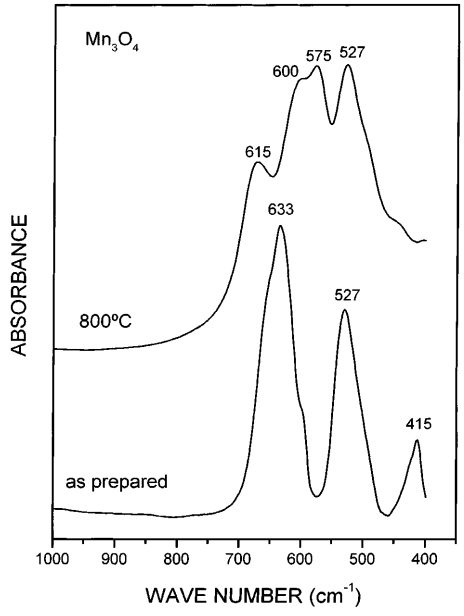

Fig. 4 IR spectra of the Mn_3O_4 sample shown in Fig. 1A, as prepared and after heating at 800 °C

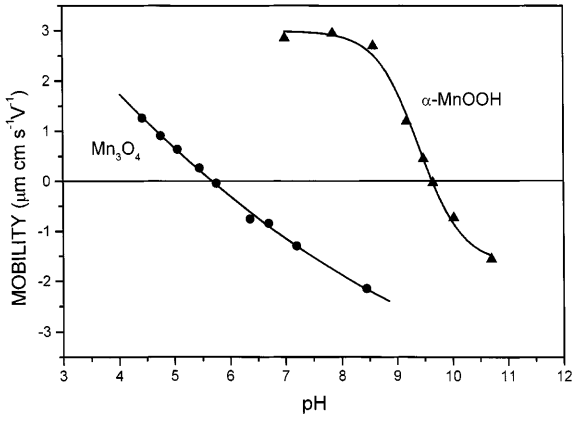

Fig. 5 Electrophoretic mobility measurements for the Mn_3O_4 and α-MnOOH samples

bands at 615, 600, 575 and 527 cm^{-1} due to bixbyite [15, 22]. After this treatment, the particles lost their equiaxial shape as a consequence of sintering (Fig. 1B).

The TGA curve of the α-MnOOH sample showed a 15% weight loss between 25 and 600 °C which took place in several consecutive steps. X-ray diffraction (Fig. 7) revealed several compositional and structural changes in the sample during this heat treatment. After annealing at 250 °C, a mixture of γ-MnO2 (ramsdellite) [23] and β-MnO_2 (pyrolusite) [24] was detected, indicating the oxidation of groutite, which agrees with the thermal behavior previously reported for this phase [8]. It should be noted that the X-ray diffraction pattern remained unaltered after heating at 170 °C for which the

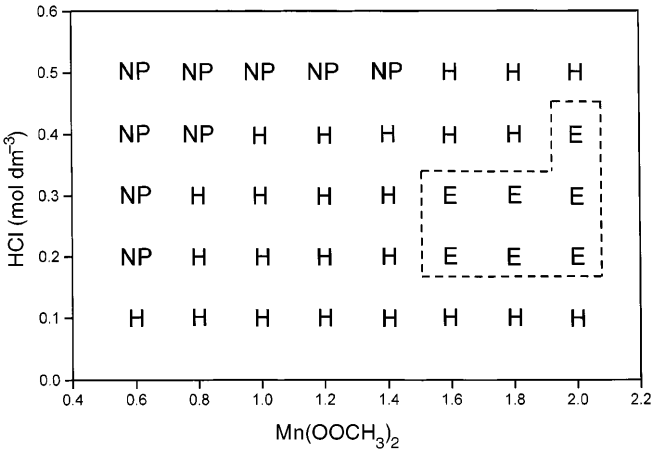

Fig. 6 Precipitation domain obtained for $Mn(OOCH_3)_2$ solutions aged at 80 °C for 24 h in the presence of variable amounts of HCl. *NP* = no precipitation, *H* = heterogeneous systems, *E* = elongated particles

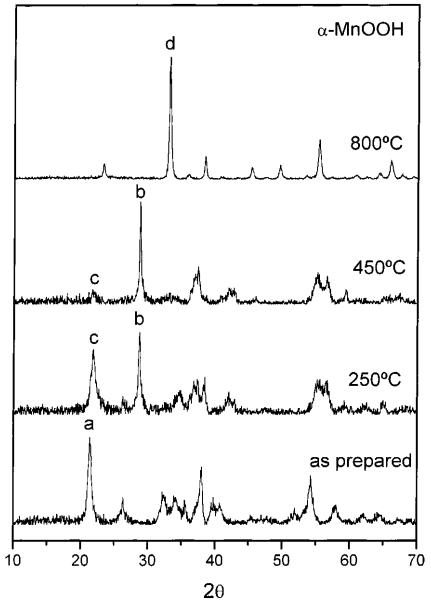

Fig. 7 X-ray diffraction patterns of the α-MnOOH sample shown in Fig. 1C, as prepared and after heating at different temperatures. *Symbols* designating the most intense peaks of different phases: *a* = α-MnOOH, *b* = MnO_2 (pyrolusite), *c* = MnO_2 (ramsdellite) and = *d* Mn_2O_3

initial weight loss (about 4%) may be mainly attributed to water desorption. As expected from previous observations [4], a phase change from ramsdellite to pyrolusite was detected at 450 °C. Finally, pyrolusite was reduced to Mn_2O_3 (bixbyite), which was the only crystalline phase observed by X-ray diffraction at 800 °C. These changes were also detected by IR spectroscopy (Fig. 8). Thus, the absorptions corresponding to the OH groups almost disappeared in the

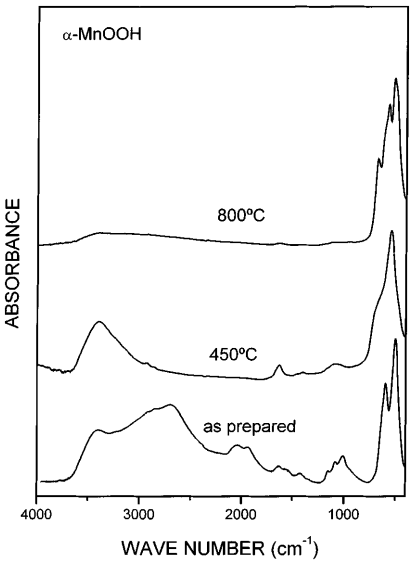

Fig. 8 IR spectra of the α-MnOOH sample shown in Fig. 1C, as prepared and after heating at different temperatures

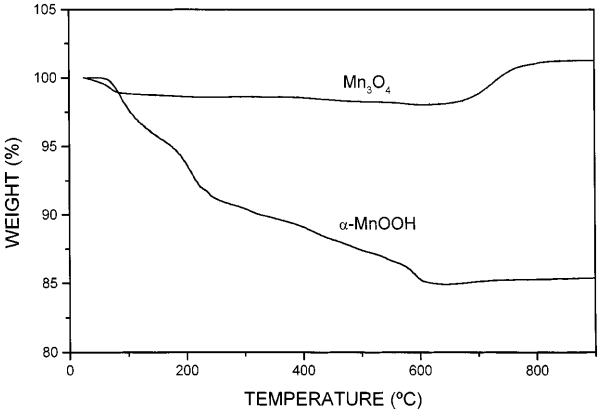

Fig. 9 Thermogravimetric curves obtained for the Mn_3O_4 and α-MnOOH samples

spectrum of the sample heated at 450 °C, which showed a strong band at 530 cm^{-1} and a shoulder at 635 cm^{-1} in the lattice vibration region due to pyrolusite [15, 25]. Finally, the spectral features of the sample heated at 800 °C were consistent with those of bixbyite [15, 22]. As a consequence of this calcination treatment some porosity was developed in the particles, although they still retained their elongated shape (Fig. 1D).

Discussion

One of the most used methods for the preparation of particles with controlled particle size and shape is the forced hydrolysis of metal cations. It has been amply reported that the morphology of the so-precipitated

particles is strongly influenced by the nature of the anions present in solution [6]. In some cases they are incorporated into the solid phase; in others, they end up adsorbed on the particle surface and can be further eliminated by washing [6]. In the last case, the effects of the anions has been mainly attributed to the formation of soluble complexes which act as precursors to the solid-phase formation [6].

In this report it has been demonstrated that the forced hydrolysis of aqueous $Mn(OOCH_3)_2$ solutions yields equiaxial nanoparticles of Mn_3O_4 or elongated α-MnOOH particles under certain experimental conditions. It is important to note that no precipitation could be detected when $Mn(OOCH_3)_2$ was substituted by other Mn(II) salts (nitrate, sulfate, chloride) and keeping constant the other experimental parameters, indicating that although the acetate anions are not incorporated to the solid phase, their presence is essential for particle formation. Similar behavior has been reported for the precipitation of small Co_3O_4 cubes from cobalt(II) acetate aqueous solutions [26]. In this case, the role of the acetate anions was tentatively attributed to solute complexation and pH regulation, although it was not clarified whether these processes affected the oxidation of Co(II) to Co(III) or the nucleation stage or both. In our case, the presence of acetate anions indeed affects the pH of the Mn(II) solutions. Thus, the pH measured before and after aging for the solution used for the precipitation of the sample shown in Fig. 1A, 0.04 mol dm^{-3} $Mn(OOCH_3)_2$, was 7.25 and 6.62, respectively, whereas the values corresponding to a manganese(II) sulfate solution aged under the same conditions were 5.48 and 5.44. However, precipitation was not detected if the initial pH of the latter solution was increased to the value corresponding to the manganese(II) acetate solution (7.25) by the addition of ammonia. It should also be noted that the initial–final pH values for the $Mn(OOCH_3)_2$–HCl solution involved in the preparation of the α-MnOOH sample were similar (5.44–5.39) to those of the manganese(II) sulfate solution. These findings suggest that the main role that acetate anions play in the precipitation of Mn_3O_4 or α-MnOOH is not related to pH control.

It is well known [27] that Mn(II) ions are very stable in acidic or neutral solutions in which they form soluble hexaaqua complexes. Only in basic media does the precipitation of $Mn(OH)_2$ take place. However, Mn(III) ions readily hydrolyze, even in acidic solutions, giving rise to precipitation [27]. These facts can explain the precipitation of α-$Mn(OH)_2$ from $Mn(OOCH_3)_2$–HCl solutions since the pH value during the aging period was in the acidic range (5.44–5.39). The formation of a mixed Mn(II)/Mn(III) compound (Mn_3O_4) from solutions only containing $Mn(OOCH_3)_2$ can be also understood since the pH range in this case was slightly basic at the beginning of the aging (7.25) and slightly acidic at the end(6.62). According to this explanation, it seems that acetate anions promote the oxidation of Mn(II) to Mn(III) in the systems reported here, which accounts for the formation of the solid phases reported. In the absence of these anions, such oxidation does not take place, for which the procedures previously reported for the precipitation of uniform particles of Mn(II) compounds from manganese(II) sulfate solutions required the addition of base or urea, which on heating decomposed, thus increasing the pH [12, 13]. The precipitation of $Mn(OH)_2$ when ammonia was added to the manganese(II) sulfate solution described previously after aging at 80 °C for 2 h was in agreement with this behavior.

Conclusions

Uniform Mn_3O_4 nanoparticles (about 20 nm) can be prepared by aging aqueous $Mn(OOCH_3)_2$ solutions under a very restrictive range of salt concentration (0.2–0.4 mol dm^{-3}) at 80 °C for 2 h. If highly concentrated solutions (1.6–2 mol dm^{-3}) are aged for longer times (24 h) in the presence of certain amounts of HCl (0.2–0.3 mol dm^{-3}), elongated α-MnOOH particles with length 2 μm or less and width 0.4 μm or less are obtained. The role that acetate anions play in the precipitation of these solids is tentatively attributed to their ability to promote the oxidation of Mn(II) to Mn(III), which readily hydrolyze causing precipitation. The Mn_3O_4 particles transform to Mn_2O_3 upon calcination at 800 °C, which is accompanied by a sintering process. The α-MnOOH sample also experiences several phase transformations on heating. First, it is oxidized at low temperature (250–450 °C) giving MnO_2 (pyrolusite), which is further reduced to Mn_2O_3 at 800 °C. After this process the particles retain their elongated shape.

Acknowledgements This work was supported by the Spanish DGICYT under project no. PB95–225. The technical assistance of Immaculada R. Cejudo is acknowledged.

References

1. Bezouhanova C, Al-Zihari MA (1992) Appl Catal A 83:45–49
2. Yongnian Y, Ruili H, Lin C, Jiayu Z (1993) Appl Catal A 101:233–252
3. Brock SL, Duan N, Rong Tian Z, Giraldo O, Zhou H, Suib SL (1998) Chem Mater 10:2619–2628
4. Vosburgh WC (1959) J Electrochem Soc 106:839–845
5. Cordoba De Torresi SI, Gorenstein A (1992) Electrochim Acta 37:2015–2019

6. Matijević E (1986) Langmuir 2:12–20
7. Gleiter H (1989) Prog Mater Sci 33:223–315
8. Moore TE, Ellis M, Selwood PW (1950) J Am Chem Soc 72:856–866
9. Mendelovici E, Sagarzazu A (1988) Thermochim Acta 133:93–100
10. Al Sagheer FA, Hasan MA, Pasupulety L, Zaki MI (1999) J Mater Sci Lett 18:209–211
11. Arul Dhas N, Koltypin Y, Gedanken A (1997) Chem Mater 9:3159–3163
12. Hamada S, Kudo Y, Okada J, Kano H (1987) J Colloid Interface Sci 118:356–365
13. Haq I, Matijević E, Akhtar K (1997) Chem Mater 9:2659–2665
14. ASTM File 24-734
15. Nohman AKH, Zaki MI, Mansour SAA, Fahim RB, Kappenstein C (1992) Thermochim Acta 210:103–121
16. Haq I, Matijević E (1997) J Colloid Interface Sci 192:104–113
17. ASTM File 24-713
18. Kohler T, Armbruster T, Libowitzky E (1997) J Solid State Chem 133:486–500
19. Nakamoto K (1986) Infrared and Raman spectra of inorganic and coordination compounds. Wiley, New York, p 232
20. Parks GA (1965) Chem Rev 65:177–195
21. ASTM File 31-825
22. White WB, Keramidas VG (1972) Spectrochim Acta Part A 28:501–509
23. ASTM File 7-222
24. ASTM File 24-735
25. Potter RM, Rossman GR (1979) Am Mineral 64:1119–1218
26. Sugimoto T, Matijević E (1979) J Inorg Nucl Chem 41:165–172
27. Cotton FA, Wilkinson G (1988) Advanced inorganic chemistry. Wiley, New York, pp 698–703